
APPLIED ELECTROCHEMISTRY
AND CORROSION PROTECTION OF METALS

Kinetics and Mechanism of Gallium Discharge and Ionization in an Alkaline Solution of Potassium Fluoride

L. F. Kozin and A. V. Gaidin

Vernadskii Institute of General and Inorganic Chemistry, National Academy of Sciences of Ukraine, Kiev, Ukraine

Received April 17, 2008

Abstract—Mechanism of gallium discharge and ionization on a liquid gallium electrode in a fluoride-alkaline electrolyte was studied. The exchange currents, transfer coefficients in the cathodic and anodic processes, and the activation energy of the electrode process were determined. The conditions in which gallium(I) ion-intermediates are formed were analyzed. The coordination numbers of the gallium complexes formed in alkaline fluoride solutions were calculated.

DOI: 10.1134/S1070427209030124

High-purity gallium finds wide application in synthesis of semiconductor compounds, instrument making, automated systems, and laser and infrared technology [1–3]. Gallium is commonly purified to remove accompanying impurities not only by chemical methods, but also by multiple-stage electrochemical techniques, which most frequently include four stages. These techniques are widely employed for deep purification of indium, gallium, lead, tin, cadmium, and bismuth [1].

In the case of gallium, the difference in the anodic and cathodic current efficiencies in each stage of electrolysis creates an imbalance with respect to the metal being refined (gallium ions in the electrolytes of the sections) and to the metal (gallium) in matrices of the bipolar (liquid gallium) electrodes. As a rule, the anodic current efficiencies by gallium exceed 100%, while the cathodic current efficiencies do not reach even 80–90% [4–6]. The latter is due both to the low overvoltage of hydrogen evolution [7] and to redox reactions between Ga(III) ions and metallic gallium, with Ga(I) intermediates, $[\text{Ga}(\text{OH})_2]$ (equivalent to $\text{Ga}[\text{Ga}(\text{OH})_4]$), formed, and to the interaction of these intermediates with oxidizing agents (H_2O , O_2 , OH^- , etc.) [1, 5]. Therefore, the principal requirement to the cyclicity of the anodic and cathodic processes in gallium refining with bipolar electrodes is that the

cathodic and anodic reactions with gallium should be reversible. Particular pronounced differences between the anodic and cathodic reactions of gallium are observed in acid and alkaline electrolytes [1]. To raise the electrochemical reversibility of the anodic and cathodic reactions of gallium in alkaline electrolytes, gallium and potassium fluorides, GaF_3 and KF , are used in the present study as activating agents.

EXPERIMENTAL

The kinetics and the mechanism of discharge and ionization of liquid gallium in fluoride-alkaline electrolytes were studied by measuring polarization curves in a thermostated three-electrode electrochemical cell equipped with a Luggin capillary. The potential of the gallium electrode was measured relative to a silver chloride reference electrode, with the values obtained reduced to the standard hydrogen electrode. Polarization studies were carried out with a P-5827 potentiostat, with curves recorded with a KSP-4 recorder from low to high current densities. The potential sweep rate was 6 mV s^{-1} . Liquid gallium of purity 99.9999% served as an electrode (surface area 0.89 cm^2). A platinum wire ($d = 1 \text{ mm}$) was used as a contact metal. The solutions used in the study were prepared from twice-distilled water and GaF_3 , KOH , and $\text{KF} \cdot \text{H}_2\text{O}$ of chemically pure grade. The measu-

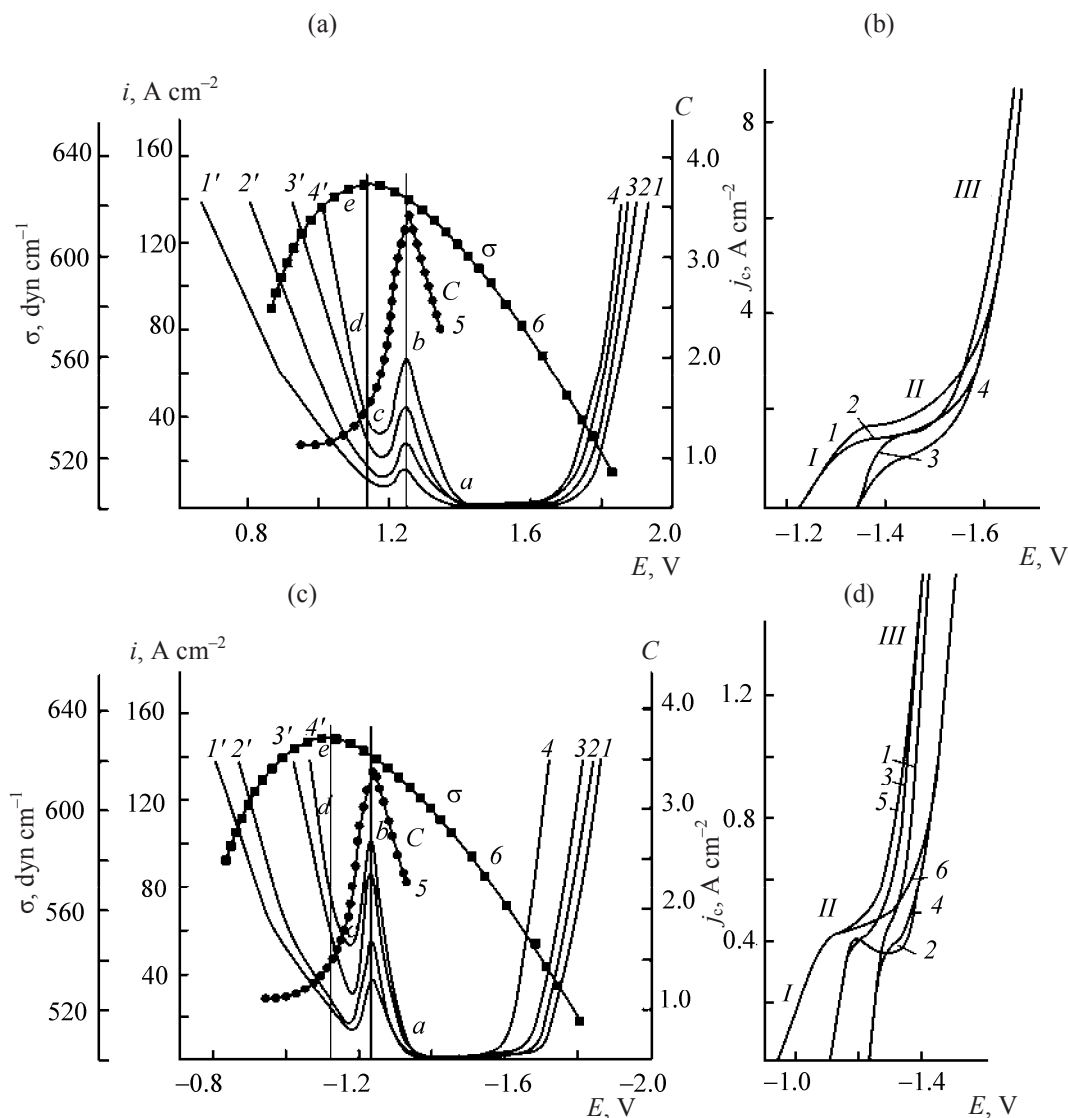


Fig. 1. Potentiodynamic polarization curves obtained on a liquid Ga electrode under various conditions. (σ) Surface tension [12], (i) current density [10], (j_c) cathodic current density, and (C) capacitance of the electrical double layer [11]. Agitation rate of the liquid Ga electrode, $\omega = 90$ rpm. (a, c) Curves: (1–4) cathodic, (1'–4') anodic, (5) C – E dependence [11], and (6) σ – E dependence [12]. T (K): (1, 1') 303, (2, 2') 313, (3, 3') 323, and (4, 4') 333. Solution composition (M): (a, c) KOH 7.0, (a) GaF₃ 0.75, (c) GaF₃ 0.15. (b, d) Data of [10, 13–15]. (b) (1–4) Cathodic curves obtained at rotation rates of (1, 3) 2600 and (2, 4) 500 rpm. Solution composition (M): (1, 2) KGaO₂ 0.22, KOH 0.6; (3, 4) KGaO₂ 1.12, KOH 2.9. (d) Cathodic curves obtained in solutions of compositions (M): (1, 2) KGaO₂ 0.1, KOH 0.07; (3, 4) KGaO₂ 0.01, KOH 0.007; and (5, 6) KGaO₂ 1 10⁻⁴, KOH 7 10⁻⁵.

rements were made at temperatures in the range 303–333 K.

Prior to measuring the polarization curves, the volume of the electrochemical cell was preliminarily purged with hydrogen to remove oxygen for 30 min and the working solutions were bubbled with hydrogen for the same purpose during the same time and then were brought in contact with the gallium electrode. The polarization curves were measured 10 min after

the cell was filled with the electrolyte, under continuous agitation of the gallium electrode and the solution with a paddle stirrer at a rate of 80 rpm.

Figure 1 shows cathodic and anodic polarization curves (PCs) obtained on a liquid gallium electrode at 303–333 K in the following solutions: (a) 7.0 M KOH + 0.75 M GaF₃ and (c) 7.0 M KOH + 2.5 M KF + 0.15 M GaF₃. As can be seen in Figs. 1a and 1c, the run of the cathodic PCs in the fluoride-alkaline electrolyte is

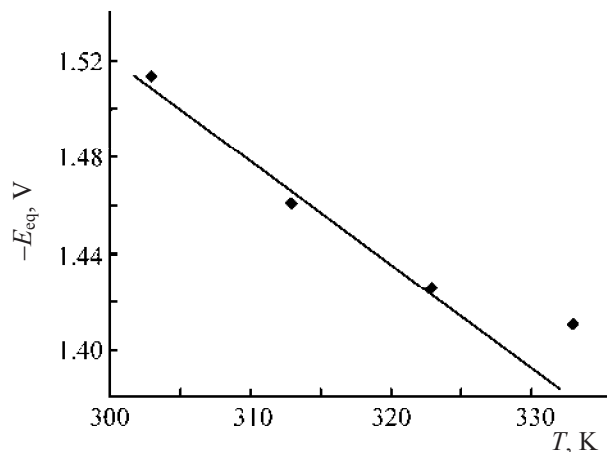


Fig. 2. Equilibrium potential E_{eq} of gallium vs. temperature T in a fluoride-alkaline electrolyte.

smooth. At the same time, the anodic PCs exhibit a complex *S*-shaped run caused by the effect of the zero-charge potential $E_{z.c}$ of gallium (ZCP) on the electrochemical kinetics [8]. The ZCP is -0.69 V (relative to s.h.e.) in 8×10^{-3} M HClO_4 [9] and -0.63 V [8] in a solution with pH 1. It should be noted that the *S*-shaped behavior run of the cathodic curves and the complex run of the capacitance curves of the gallium electrode were observed in numerous studies [10–15]. However, the interpretation of this experimental fact was different from that in [16–20].

Analysis of the data of [12–15] demonstrated that the depth of bends and, consequently, the values of $E_{z.c}$ depend on the nature of the electrolyte (acid or alkaline) and the solution components. The pronounced shift of the potentials of the bends in the run of the PCs in the negative direction in concentrated halide solutions in the systems $\text{M}|\text{MX}_n$ ($X = \text{H}_2\text{SO}_4$, OH^- , Cl^- , Br^- , I^- , etc.; $\text{M} = \text{Mn}$ [16, 17], Cd , Tl , Pb [18, 19], Bi , Sn , Sb , Cd , Ga , In , and Ag [20]) is due, as shown in [16–20], to the effect of the ZCP on the run of PCs.

However, the shift of the ZCP in the case of gallium in halide and, especially, alkaline solutions lags behind the shift of the equilibrium potential of gallium. Because of the formation of hydroxide-containing complexes, intermediates, and gallium hydrides, the potential $E_{z.c}$ of gallium in alkaline solutions must lie to the left of the peak in the electrocapillary curve of gallium. The observed values of $E_{z.c}$ of gallium depend on the electrolyte nature and, therefore, may fall within the range of potentials of both anodic (Figs. 1a, 1c; alkaline solutions) and

cathodic polarization curves (Figs. 1b, 1d; acid solutions).

The bends in the cathodic PCs of gallium were attributed in [12] to the formation of passivating layers composed of “difficultly soluble oxides and hydroxides of Ga with various valences” on the gallium surface. However, this statement contradicts a conclusion of the same authors that the “cathodic process occurs with the minimum overvoltage” and “metallic Ga is deposited at the electrode.” In [12], the bends in the PCs could be eliminated neither by using a dropping electrode or ultrasound, nor by mechanical cleaning of the rotating electrode or solution agitation, nor by raising the electrolyte temperature. These procedures would seemingly have eliminated the passivation of gallium in the electrolysis process because of the formation of difficultly soluble compounds of “gallium with various valences.” As can be seen in Figs. 1b and 1d, bends in the PCs are observed at $E_c = -(1.2\text{--}1.28)$ V. Upon further increase in the polarization, the rate of the cathodic process steadily grows.

The equilibrium potential E_{eq} of the gallium electrode in the electrolyte under study at different temperatures is -1.513 V (303 K), -1.460 V (313 K), -1.425 V (323 K), and -1.409 V (333 K). As can be seen in Fig. 2, E_{eq} shifts toward more positive values as temperature is elevated. The isothermal coefficient of the standard potentials of gallium, $(dE^0/dT)_{\text{isotherm}} = 0.67$ mV K^{-1} [21, 22]. It follows from Fig. 2 that, in the fluoride-alkaline electrolyte, the isothermal coefficient of the equilibrium potential, $(dE^0/dT)_{\text{isotherm}} = 4.47$ mV K^{-1} .

The current peaks in the anodic PCs of gallium (Figs. 1a, 1c) appear at $E_a = -1.25$ V. As the anodic polarization increases further, the current steeply decreases along the *bc* portion and reaches the minimum value at point *c*. As the anodic polarization of the gallium electrode increases still further, the current starts to gradually grow and the electrode surface acquires a positive charge. Negatively charged OH^- and F^- ions start to be adsorbed on the positively charged surface and the anode current gradually grows, reaching values of 140 mA cm^{-2} and more at a moderate polarization.

Such a complex run of the anodic PCs may be due to the effect of $E_{z.c}$ on the exchange processes in the electrical double layer (EDL) and, as a consequence, on the kinetics and mechanism of electrode reactions.

It is known from the theory of the double layer that $E_{z,c}$ can be found from the position of a dip or a peak in differential capacitance curves [8, 23, 24] or from the peak in electrocapillary curves [11, 25, 26].

An analysis of the dependence of the differential capacitance C on the potential of the liquid and solid gallium electrodes shows that $E_{z,c} = -1.256$ V in 1 N Na_2SO_4 and $E_{z,c} = -1.25$ V in 0.1 N KOH [11].

In [24], bends in the differential capacitance curves (C,E curves) of gallium were observed at potentials of $-(1.0-1.1)$ V at high electrolyte concentrations (M): KI 0.1–2.0, LiCl 1–12, KBr 1–4, and NaClO_4 0.1–4. The formation of the breaks in the C,E curves of gallium is attributed to presence on the gallium surface of chemisorbed water dipoles with the negative end facing the metal. Therefore, the orientation of water dipoles changes upon incorporation of anions having a polarizing capacity into the dense EDL.

Interestingly, the potentials at which bends were observed in the C,E curves of gallium in [24] coincided with the potentials of the peak in electrocapillary curves. For example, the potential of the bend coincided with $E_{z,c} = -1.125$ V of gallium in a 1 M KI + HCl solution [12], with $E_{z,c} = -1.154$ V in a 1.0 M KCl solution acidified with a KOH solution to 0.01 M [25], and with $E_{z,c} = -(0.95-1.07)$ V in diluted 0.006–0.1 M solutions of potassium chlorides, bromides, and iodides and sodium perchlorates [26]. It was found in [22] that breaks are formed in C,E curves, and the depth of these breaks depends on the electrolyte concentration. The positions of the dips in the solutions studied coincide and correspond to $E_{z,c}$ in aqueous solutions.

To gain insight into the electrochemical processes responsible for the appearance of bends in the anodic PCs (Figs. 1a, 1c), the anodic-cathodic PCs were compared with the curve describing the dependence of the differential capacitance of gallium on potential [11] and with the electrocapillary curve of gallium [12]. It can be seen that the bend potential in the PCs coincides with the potential of the maximum capacitance in the C,E curve, which corresponds to $E_{z,c} = -1.256$ V.

As the potential is shifted from point a to more positive values, the anode current increases to point b and then sharply decreases to point c (Figs. 1a, 1c). This occurs because, at point b , a potential $E_{z,c}$ is reached whose region extends both to the left and to the right of point $E_{z,c}$.

At $E_{z,c}$ the surface has zero charge. It can be assumed that, at the point $E_{z,c}$, negative charges flow to positive charges and are mutually neutralized. As shown in [12, 24], water dipoles are chemisorbed on gallium at low surface charges, with the negative charge of oxygen oriented toward metallic gallium. In this case, the electrical resistance of the near-electrode double layer (NDL) markedly increases, and, as a result, the anode current sharply decreases along portion bc . Apparently, the EDL becomes dielectric at point c . If it is assumed that the space between the positive surface charges e^+ to the left of the zero-charge point and negative charges e^- to the right of the $E_{z,c}$ point is separated by a nonconducting medium, adsorbed water molecules in the case in question, then the electric field strength $E_{e,f}$ will be given by the known equation

$$E_{e,p} = e^+e^-/(\epsilon h^2), \quad (1)$$

where ϵ is the dielectric constant of distilled water, equal to 32 [27]; and h is the distance between the charges.

An approximate analysis shows that $E_{e,f} \ll 1$ near $E_{z,c}$. This leads to a sharp decrease in the anode current in bc region for the gallium electrode (Figs. 1a, 1c).

Depending on the charge of the surface of the gallium electrode, oppositely charged solution components (cations or anions) are adsorbed. As can be seen in Figs. 1a and 1c, as the potential of the gallium electrode is shifted to more electropositive values, the anode current starts to grow (cde region), the electrode surface gradually becomes positive, and, as a consequence, OH^- and F^- ions start to be adsorbed. The electrode process of gallium ionization to give intermediates, Ga^+ ions, occurs more intensively [28, 29]. On being formed, these positively charged Ga^+ ions are repulsed from the positively charged surface of the gallium electrode, are transferred beyond the limits of the EDL, and, after the equilibrium concentration is reached, undergo disproportionation (DPP) in accordance with the equation



Depending on the rate constant dependent on the nature of the electrolyte, the DPP reaction may occur within the EDL or in the solution bulk [28, 29].

As the anodic polarization increases, the electric field strength in the EDL within the near-electrode layer at the positively charged surface of the gallium electrode grows. As a consequence, negatively charged

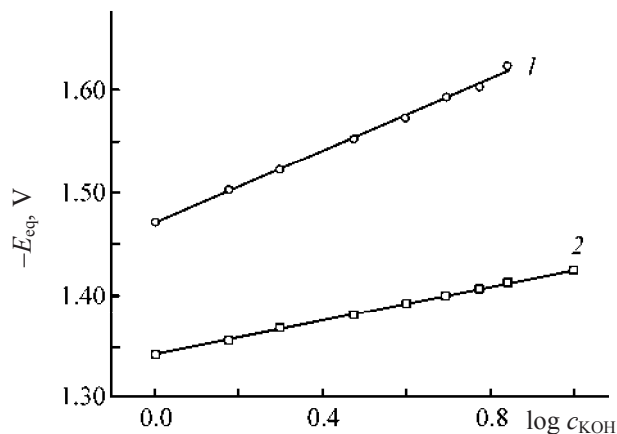


Fig. 3. Equilibrium potential E_{eq} of the liquid Ga electrode vs. the KOH concentration c_{KOH} in a solution of composition 0.15 M $GaF_3 + x$ M KOH at a temperature of 30°C. Agitation rate $\omega = 80$ rpm. (1) Experimental values and (2) values calculated for $z_{OH^-} = 1$.

OH^- and F^- ions are adsorbed and consumed in steadily increasing amounts. In the end, well soluble fluorohydroxo complexes of gallium are formed, no hindrance to the anodic process is observed, and the anode current reaches large values (Figs. 1a, 1c; *de* region).

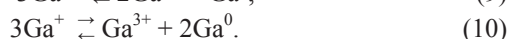
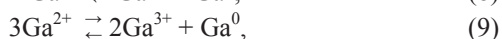
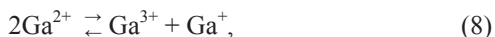
At potentials more negative than the equilibrium potential of gallium $-(1.631-1.735)$ V, the electrode surface is negatively charged and gallium(III) ions are adsorbed on this surface. The ions may be involved in the electrochemical reaction of stage-by-stage



or heterostage reduction [28, 29]

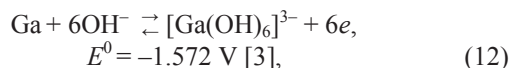


to give intermediates, Ga^{2+} and Ga^+ ions. Ga^{2+} ions may also be involved in DPP reactions in accordance with the equations



The chemical nature of the DPP reactions was considered in detail in [28, 29].

In alkaline solutions with a high content of an alkali, the potential-determining reactions are the following

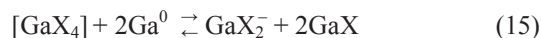
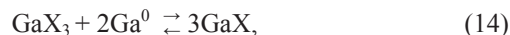


The equilibrium potential E_{eq} of reaction (11) can be calculated by the equation [30]

$$E_e = E^0 + \frac{2.303RT}{zF} \log [Ga(OH)_4]^- - 0.0786 \log [OH^-], \quad (13)$$

where E^0 is the standard electrode potential of gallium(III); z , number of electrons involved in the reaction ($z = 3$); R , universal gas constant; T , temperature; and F , Faraday number.

As shown in [1, 4, 28, 29, 31–35], the contact of gallium ions of the highest valence with metallic gallium can yield by the reproportionation (RPP) reaction



gallium(I) monohydroxides and monofluorides or their mixed compounds [36–39]. For example, in contact of gallium trihydroxo fluoride $[Ga(OH)_3F]^-$ or gallium tetrafluoride $[GaF_4]^-$ with metallic gallium, the RPP reaction [Eq. (15)] will give $2GaF$, or $2[Ga(OH)F]^-$, or $2Ga(OH)^-$.

Figure 3 shows the dependence of the equilibrium potential of gallium in a fluoride-alkaline solution on the KOH concentration. The experimental points well fall on the straight line $E_{eq}-\log [KOH]$ (curve 1). The calculated dependence $E_{eq}-\log [KOH]$ at $z_{OH^-} = -1$ for solutions of the above composition at 30°C is represented by a straight line with a slope of 0.0601 V ($T = 303$ K) (Fig. 3, curve 2).

The coordination number p of gallate gallium(III) ions in solution was calculated using the equation [40]:

$$p = \frac{zF\partial E_e}{2.303RT\partial \log c_{OH^-}}, \quad (16)$$

where $z = z_{OH^-} = -1$, and c_{KOH} is the KOH concentration in the electrolyte (M).

An analysis of the data obtained demonstrated that

$$\frac{\partial E_e}{\partial \log c_{OH^-}} = 0.183 \text{ V}$$

and the calculated coordination number for $z_{OH^-} = -1$ is 3.04. Consequently, gallium complexes comprising three OH^- groups are formed in the bulk of the

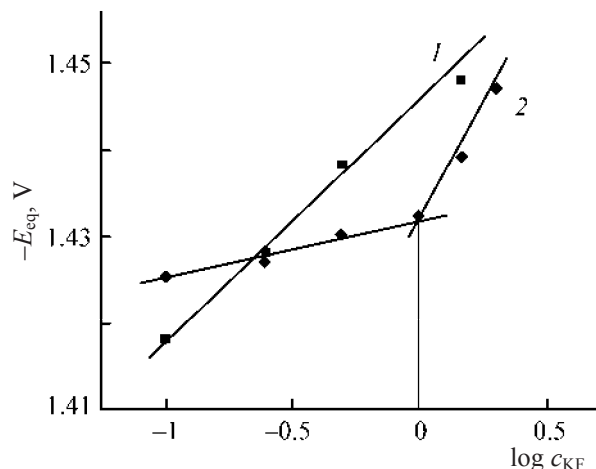


Fig. 4. Equilibrium potential E_{eq} of the liquid Ga electrode vs. the KF concentration c_{KF} in solutions of various compositions. Solution composition (M): (1) KOH 7.0, GaF_3 1×10^{-3} , KF x ; (2) KOH 7.0, GaF_3 1×10^{-2} , KF x .

electrolyte. Because F^- ions are also present in the electrolyte, mixed compounds of gallium can be formed, too [36–39].

Figure 4 shows how the equilibrium potential of the liquid gallium electrode depends on $\log c_{KF}$ in a 7.0 KOH + 0.0001 M GaF_3 + x M KF solution at 303 K (curve 1). It can be seen that the E_{eq} – $\log c_{KF}$ dependence is linear. The coordination number p of F^- ions was calculated by the equation [40]:

$$p = \frac{z_F F \partial E_e}{2.303 RT \partial \log c_{KF}}, \quad (17)$$

where $z_F = -1$ and c_{KF} is the KF concentration (M).

It was found that the coordination number p is 0.5 for this solution (Fig. 4, curve 1). The dependence of the equilibrium potential of gallium on $\log c_{KF}$ in a solution of composition 7 M KOH + 0.01 M GaF_3 + x M KF is shown in Fig. 4, curve 2. In this case, the coordination number calculated by Eq. (17) is 0.998, i.e., is close to unity.

Mononuclear hydroxo complexes of gallium(III) have the following stability constants: $[Ga(OH)]^{2+}$ – $\log \beta_1 = 11.19$, $[Ga(OH)_2]^+$ – $\log \beta_2 = 21.68$, $[Ga(OH)_3]$ – $\log \beta_3 = 31.65$, $[Ga(OH)_4]^-$ – $\log \beta_4 = 38.84$, and $[Ga(OH)_6]^{3-}$ – $\log \beta_6 = 40.30$ [41, 42].

Accordingly, the stability constants of mononuclear complexes of gallium(III) in fluoride complexes are as follows: GaF^{2+} – $\log \beta_1 = 6.19$, GaF_2^+ – $\log \beta_2 = 10.72$, GaF_3 – $\log \beta_3 = 13.49$, and $[GaF_4]^-$ – $\log \beta_4 = 14.52$ [42]. Comparison of $\log \beta_n$ of Ga(III) in fluoride solutions

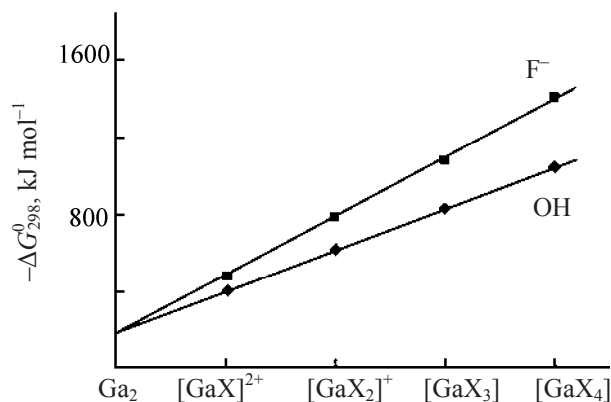


Fig. 5. Change in the Gibbs energy, ΔG_{298}^0 , in the formation of fluoride and hydroxide complexes of gallium(III). Data from the reference book [41].

with $\log \beta_n$ of hydroxo complexes in alkaline solutions shows that the fluoride complexes are less stable.

Figure 5 shows data on changes in the Gibbs energy in the formation of gallium(III) fluorides and hydroxides $[GaX]^{2+}$, $[GaX_3]$, and $[GaX_4]^-$, taken from the reference book [41]. The data in Fig. 4 can be used to calculate the equilibrium constants in the binary systems $mGa^{3+} - xF^-$ and $nGa^{3+} - yOH^-$. Therefore, it can be assumed, in view of the determined coordination numbers $p_{OH^-} = 3$ and $p_{F^-} = 1$, that mixed hydroxo complexes of composition $[Ga(OH)_3F]^-$ are formed in the fluoride-alkaline solution [36–39]. The overall stability constant of the mononuclear mixed complex formed in accordance with the equation

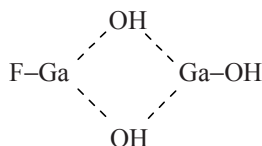


can be calculated by the formula [42]

$$\beta_{OH^-, F^-} = \frac{[Ga(OH)_3F]K}{[Ga^{3+}][OH^-]^3[KF]}. \quad (19)$$

The mixed complex $[Ga(OH)_3F]K$ from reaction (18) is formed by the mechanism of step-by-step complexation, with the concentrations of OH^- and F^- varying “from 0 to the maximum ligand number” [42].

In the fluoride-alkaline solution of gallium fluoride, RPP reactions (6), (14), and (15) to give Ga(I) intermediates ($GaOH$, $[Ga(OH)_2]^-$, GaF , $[GaF_2]^-$) are possible. When gallium intermediates are produced in solution, binuclear gallium complexes can be formed, e.g.,



In this case, the stability constant of the mixed binuclear complex can be calculated by the equation

$$\beta_{\text{OH}^-, \text{F}^-} = \frac{[\text{Ga}(\text{OH})_3\text{F}]\text{Ga}}{[\text{Ga}^{3+}][\text{OH}^-]^3[\text{F}^-][\text{Ga}^+]}. \quad (20)$$

The most difficult in analysis of equilibria in systems with gallium(I) intermediates is the determination of their concentration because of the high reactivity of the intermediates Ga^- , Ga^+ , Ga^{2+} , Ga^{2+} toward H^+ ions, H_2O , atmospheric oxygen, etc. The standard potentials of gallium in the formation of the lowest valence ions are more positive ($E_{\text{Ga}^+/\text{Ga}}^0 = -0.406$ V and $E_{\text{Ga}^{2+}/\text{Ga}}^0 = -0.452$ V [28, 29]) than $E_{\text{Ga}^{3+}/\text{Ga}}^0$. Therefore, the initial equilibrium potential $E_{\text{Ga}^{3+}/\text{Ga}}$ is shifted to more positive values in the polarization of the gallium electrode in the fluoride-alkaline solution because of the formation of the potential-determining ions Ga^+ and Ga^{2+} . The potential difference ΔE_i is 0.2008 V in the formation of Ga^+ ions and $\Delta E_i = 0.101$ V in the system $\text{Ga}^{3+}/\text{Ga}^+$ [28, 29]. Therefore, $E_{\text{Ga}^{3+}/\text{Ga}} = -1.313$ V and $E_{\text{Ga}^{3+}/\text{Ga}^+} = -1.614$ V in the fluoride-alkaline solution under study.

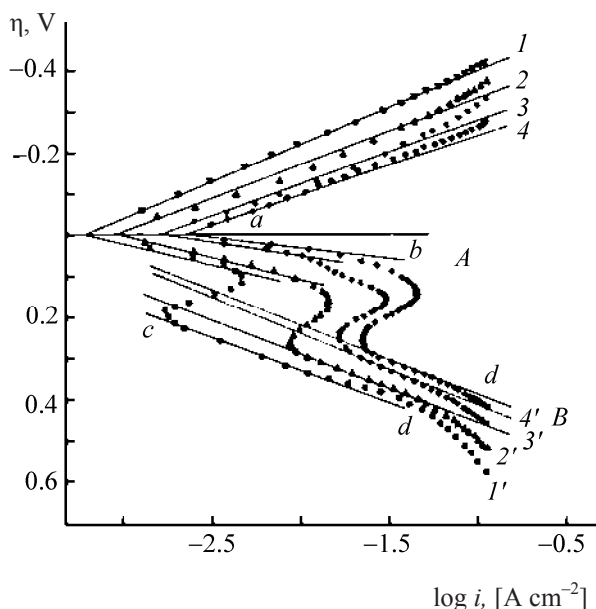


Fig. 6. Overvoltage η of (1–4) discharge of gallium(III) ions and (1'–4') ionization of metallic gallium on a liquid Ga electrode in a solution of composition 7.0 M KOH + 2.5 M KF + 1×10^{-3} M GaF_3 vs. the current density i . T (K): (1, 1') 303, (2, 2') 313, (3, 3') 323, and (4, 4') 333.

Figure 6 shows how the overvoltage of gallium discharge-ionization at a liquid gallium electrode depends on the logarithm of the current density in the fluoride-alkaline solution of composition (M): KOH 7.0, KF 2.5, and GaF_3 1×10^{-3} . It can be seen that the cathodic dependences obtained, $\eta_c - \log i_c$, are linear in a wide range of current densities. The anodic polarization curves show S-shaped bends similar to those in Figs. 1a and 1c and two linear portions A and B. Portions A and B are for the ranges of low and high anode current densities, respectively. An S-shaped region resulting, as shown above, from the effect of $E_{z,c}$ on the PCs lies between portions A and B. The linear portions in the $\eta_i - \log i_i$ made it possible to find the exchange currents in accordance with the Tafel equations for the cathodic and anodic processes:

$$\eta_c = \frac{2.303RT}{\alpha z_c F} \log i_0 + \frac{2.303RT}{\alpha z_c F} \log i_c, \quad (21)$$

$$\eta_a = \frac{2.303RT}{\alpha z_a F} \log i_0 + \frac{2.303RT}{\alpha z_a F} \log i_a, \quad (22)$$

where α , β are the transfer coefficients in the cathodic and anodic processes; i_e , exchange current (A cm^{-2}); and z_c and z_a , numbers of electrons involved in the cathodic and anodic processes.

The dependences $\eta_i - \log i_i$ (Fig. 6) were used to graphically determine the slope for the cathodic (b_c^e) and anodic (b_a^e) portions A and B at various temperatures (see table). The table also lists the exchange currents, kinetic parameters, and charge transfer coefficients for gallium discharge-ionization on a liquid gallium electrode in a fluoride-alkaline solution at temperatures of 303–333 K.

As can be seen in the table, the slope ratios of the cathodic (b_c^e) and anodic (b_a^e) processes at low current densities (portion A) decrease as temperature is elevated.

The charge transfer coefficients were calculated by the equations

$$\alpha^e = \frac{2.303RT}{b_c^e z_c F}, \quad \beta^e = \frac{2.303RT}{b_a^e z_a F}, \quad (23)$$

using the experimental values of b_c^e and b_a^e , listed in the table.

The theoretical values of the slope for the cathodic transport of electrons at $z = 1$ and temperatures of 303, 313, 323, and 333 K are 0.120, 0.124, 0.128, and 0.132 V, respectively. The theoretical values of the charge transfer coefficients for slow discharge, $\alpha = \beta = 0.5$.

Kinetic parameters of the electrode process of discharge–ionization of a liquid gallium electrode in solutions of compositions (M): 7.0 M KOH + 0.15 M GaF₃ (solution 1) and 7.0 M KOH + 2.5 M KF + 1×10^{-3} M GaF₃ (solution 2) at various temperatures ($E_a = 43.83 \text{ kJ mol}^{-1}$)

$T, \text{ K}$	$E_{\text{eq}}, \text{ V}$	$b_c^e, \text{ V}$	$b_a, \text{ V}$	α^e	β^e	$b_a^e, \text{ V}$	β^e	$i_0, \text{ A cm}^{-2}$
	Solution 1 ^a					Solution 2 ^b		
303	–1.513	0.160	0.107	0.43	0.56	0.156	0.38	4.68×10^{-4}
313	–1.460	0.149	0.083	0.45	0.55	0.169	0.37	8.91×10^{-4}
323	–1.425	0.126	0.054	0.48	0.52	0.174	0.37	2.56×10^{-4}
333	–1.409	0.107	0.043	0.56	0.44	0.176	0.37	1.41×10^{-3}

^a For the anodic potential range at low current densities (portion A).

^b For the anodic potential range at high current densities (portion B).

Real values of α^e and β^e may deviate from the theoretical values within $\pm(10\text{--}30)\%$, but the sum $\alpha + \beta = 1.0$ [29].

As can be seen in the table, the value of α^e , calculated from experimental values of b_c^e , increases, as temperature is elevated, from 0.43 at 303 K to 0.56 at 333 K. For the anodic process, the value of β^e (portion A) decreases, as temperature is elevated from 303 to 333 K, from 0.56 at 303 K to 0.44 at 333 K. Interestingly, the sum $\alpha^e + \beta^e$ is close to unity at 303 K ($\alpha + \beta = 0.43 + 0.56 = 0.99$), and is exactly unity at 333 K ($\alpha + \beta = 0.56 + 0.44 = 1.0$). The increase in the transfer coefficient of the cathodic process (α^e), decrease in the anodic transfer coefficient β^e (portion A), and increase in b_a^e (portion B) are due to the occurrence of chemical reactions of RPP, e.g., reactions (6), (14), and (15) in the electrode process to give Ga^+ intermediates having high reactivity toward OH^- , H_2O , etc. [29].

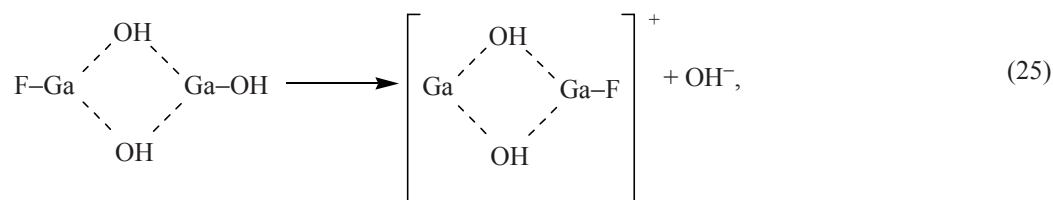
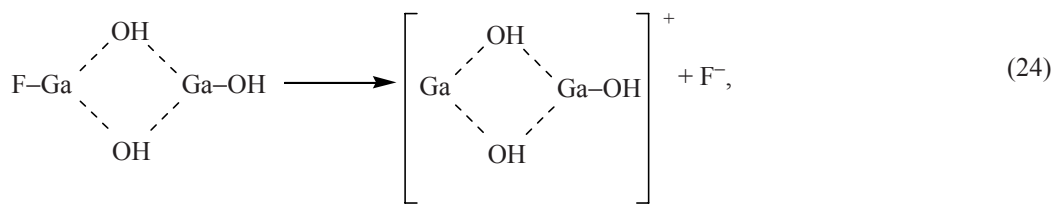
It is of interest that, for the anodic process at high current densities, the slope of the Tafel portion B (Fig. 6, region *cd*) increases as temperature is elevated, in accordance with the electrochemical theory (see table, b_a^e for portion B), even though it exceeds the theoretical values presented for the temperatures studied. In this case, the charge transfer coefficients retain a constant value close to $\beta^e = 0.4$.

Analysis of the data shows that, in the cathodic process, the rate-determining stage of the electrode process in a fluoride-alkaline electrolyte is addition of the first electron, presumably to positively charged ions, products of dissociation of the mixed complex $[\text{Ga}(\text{OH})_3\text{F}]^-$, rather than to the negatively charged molecule of this complex, because the surface of the Ga cathode is negatively charged (Figs. 1a, 1c).

It can be seen in Figs. 1a and 1c that, in the cathodic polarization of the gallium electrode in a fluoride-alkaline solution containing 0.75 and 0.15 M of GaF₃, the cathodic curve at $i_c \approx 0$ sharply shifts from the equilibrium potential E_{eq} (see table) into the region of negative potentials. Apparently, the mixed complex dissociates in the electric field of the EDL of the gallium electrode, and also in exchange reactions, to give positively charged ions of fluoride and hydroxide complexes with compositions presented in Fig. 5. The interaction of the components in the electrode–electrolyte system leads to exchange RPP reactions, ligand substitution processes, and changes in the electrode potential [43, 44]. The positive gallium species formed in this case ($[\text{GaF}]^{2+}$, $[\text{Ga}(\text{OH})\text{F}]^+$, $[\text{Ga}(\text{OH})]^{2+}$, etc.) are adsorbed on the negatively charged surface of the gallium cathode (Figs. 1a, 1c) and are involved in chemical and electrochemical reactions.

It should be noted that the presence of fluoride ions in the solution composed of 7.0 M KOH + 2.5 M KF + x M GaF₃ results in that the stability of gallium(I) ions $\{\text{GaF}, [\text{Ga}(\text{OH})\text{F}]\}$ increases and binuclear mixed Ga(I) complexes $[\text{Ga}(\text{OH})_3\text{F}]$ are formed (in accordance with the experimental evidence that $p_{\text{F}^-} = 1$ and $p_{\text{OH}^-} = 3$), which dissociate to give positively charged complex ions adsorbed on the negatively charged surface of the gallium cathode.

The temperature dependence of the exchange currents listed in the table was used to calculate the activation energy of the electrode reaction of gallium discharge and ionization, $E_a = 43.83 \text{ kJ mol}^{-1}$, which points to the kinetic control over the rate of the electrode reactions of gallium discharge–ionization in the fluoride-alkaline solution.



On the whole, the kinetic parameters obtained for the liquid gallium electrode in a fluoride-alkaline electrolyte in the temperature range 303–333 K and data on the *S*-shaped bends in anodic polarization curves indicate that both the cathodic and anodic electrode processes on gallium occur by a complex mechanism and the zero-charge potential of gallium plays an important role in these processes.

CONCLUSIONS

(1) The *S*-shaped bends observed in anodic polarization curves are due to the effect of the zero-charge potential on the course of adsorption processes on the surface of a positively charged liquid gallium electrode and, on the whole, on the kinetics and mechanism of the electrode process.

(2) Mixed trihydroxo fluoride gallium complexes $[\text{Ga}(\text{OH})_3\text{F}]^-$ are formed in fluoride-alkaline solutions, which is indicated by the calculated coordinated numbers of gallium complexes: three for hydroxy ions and unity for fluoride ions.

(3) The kinetic parameters of the liquid gallium electrode, obtained in a fluoride-alkaline electrolyte in the temperature range 303–333 K (charge transfer coefficients, slope ratios of the cathodic and anodic processes, and exchange currents), indicate that both cathodic and anodic electrode processes on gallium occur by a complex mechanism.

(4) The activation energy of the electrode process ($43.83 \text{ kJ mol}^{-1}$), calculated from the temperature dependence of exchange currents, points to kinetic limitations on the rate of the electrode reactions of gallium discharge–ionization in a fluoride-alkaline electrolyte.

REFERENCES

1. Kozin, L.F. and Volkov, S.V., *Khimiya i tekhnologiya vysokochistyykh metallov i metalloidov* (Chemistry and Technology of High-Purity Metals and Metalloids), Kiev: Naukova dumka, 2002, vol. 1.
2. Kozlov, S.A., Sazhin, M.V., Petrukhin, I.O., et al., *Naukoemk. Tekhnol.*, 2003, no. 2, p. 88.
3. Ivanova, R.V., *Khimiya i tekhnologiya galliya* (Chemistry and Technology of Gallium), Moscow: Metallurgiya, 1973.
4. Kozin, D.F., Open'ko, N.M., and Zhylykamanova, K., *Ukr. Khim. Zh.*, 1991, vol. 57, no. 2, p. 156.
5. Gaidin, A.V. and Kozin, L.F., *Nanosist. Nanomater. Nanotekhnol.*, 2006, vol. 4, no. 4, p. 1007.
6. Mikhnev, A.D., Kolmakov, A.A., and Zyablitseva, E.G., *Izv. Vyssh. Uchebn. Zaved., Tsvetn. Metall.*, 1998, no. 5, p. 24.
7. Kozin, L.F. and Gaidin, A.V., *Ukr. Khim. Zh.*, 2007, vol. 73, no. 8, p. 104.
8. Frumkin, A.N., *Potentsialy nulevogo zaryada* (Zero-Charge Potentials), Moscow: Nauka, 1982.
9. Khrushcheva, E.I. and Kazarinov, V.E., *Elektrokhimiya*, 1986, vol. 22, no. 9, p. 1262.
10. Survilene, S.P. and Vishomirskis, R.M., *Trudy Akad. Nauk LatvSSR, Ser. B*, 1983, vol. 5 (138), p. 21.
11. Leikis, D.I. and Sevast'yanov, E.S., *Dokl. Akad. Nauk SSSR*, 1962, vol. 144, no. 6, p. 1320.
12. Frumkin, A.N., Polyanovskaya, N.S., and Grigor'ev, N.B., *Dokl. Akad. Nauk SSSR*, 1964, vol. 157, no. 6, p. 1455.
13. Selekhnova, N.P., Lyubimova, N.A., and Leikis, D.I., *Elektrokhimiya*, 1972, vol. 8, no. 5, p. 721.
14. Popova, T.I. and Simonova, N.A., *Elektrokhimiya*, 1970, vol. 6, no. 9, p. 1378.
15. Popova, T.I., Simonova, N.A., Moiseeva, Z.N., and Bardina, N.G., *Elektrokhimiya*, 1970, vol. 6, no. 8, p. 1125.
16. Kozin, L.F., Mashkova, N.V., Manilevich, F.D., and Danil'tsev, B.I., *Zh. Prikl. Khim.*, 2007, vol. 80, no. 5, p. 751.

17. Kozin, L.F., Mashkova, N.V., and Manilevich, F.D., *Zashch. Met.*, 2007, vol. 43, no. 6, p. 594.
18. Kolotyркин, Ya.M. and Bune, N.Ya., *Zh. Fiz. Khim.*, 1947, vol. 21, no. 5, p. 581.
19. Kolotyркин, Ya.M. and Medvedeva, L.A., *Trudy soveshchaniya po elektrokhemii* (Proc. of Symp. on Electrochemistry), Moscow: Akad. Nauk SSSR, 1953, p. 369.
20. Rotinyan, A.L., Kilimnik, A.B., and Levin, E.D., *Dvoynoi sloi i adsorbtsiya na tverdykh elektrodakh. II. Materialy simpoziuma, Tartu, 18–21 iyunya 1970 g.* (Double Layer and Adsorption on Solid Electrolytes, II, Proc. of Symp., Tartu, June 18–21, 1970), Tartu, 1970, p. 321.
21. *Spravochnik po elektrokhemii* (Handbook of Electrochemistry), Sukhotin, A.M., Ed., Leningrad: Khimiya, 1981.
22. Milazzo, G. and Caroli, S., *Tables of Standard Electrode Potentials*, New York: John Wiley & Sons, 1978.
23. Faizullin, F.F., Nikitin, E.V., and Gudina, N.N., *Elektrokhemiya*, 1967, vol. 3, no. 1, p. 120.
24. Grigor'ev, N.B., *Elektrokhemiya*, 1967, vol. 3, no. 4, p. 511.
25. Polyanovskaya, N.S. and Frumkin, A.N., *Elektrokhemiya*, 1967, vol. 3, no. 9, p. 1129.
26. Frumkin, A.N., Grigor'ev, N.B., and Bagotskaya, I.A., *Dokl. Akad. Nauk SSSR*, 1964, vol. 157, no. 4, p. 957.
27. Kuchling, H., *Taschenbuch der Physik*, Leipzig: Fachbuchverlag im Carl Hanser Verlag, 2004.
28. Kozin, L.F., *Ukr. Khim. Zh.*, 1993, vol. 59, no. 9, p. 951.
29. Kozin, L.F., *Elektroosazhdenie i rastvorenie mnogovalentnykh metallov* (Electrodeposition and Dissolution of Polyvalent Metals), Kiev: Naukova dumka, 1989.
30. Survilene, S.P. and Vishomirskis, R.M., *Trudy Akad. Nauk LatvSSR, Ser. B*, 1983, vol. 4 (137), p. 11.
31. Survilene, S.P. and Vishomirskis, R.M., *Trudy Akad. Nauk LatvSSR, Ser. B*, 1975, vol. 4 (88), p. 51.
32. Kozin, L.F. and Egorova, A.G., *Izv. Akad. Nauk KazSSR, Ser. Khim.*, 1968, no. 3, p. 6.
33. Kozin, L.F., Sarmurzina, R.G., and Egorova, A.G., *Trudy Inst. Organ. Kataliza Elektrokhem., Akad. Nauk KazSSR*, 1975, vol. 11, p. 16.
34. Sarmurzina, R.G., *A Study of the Kinetics and Equilibrium of the Reaction of Formation of Univalent Gallium Ions in the System $Ga^0 - Ga^+ + Ga^{3+}$ in Aqueous-Salt Solutions*, Cand. Sci. Dissertation, Alma-Ata, 1973.
35. Kozin, L.F. and Egorova, A.G., *Trudy Inst. Organ. Kataliza Elektrokhem., Akad. Nauk KazSSR*, 1980, vol. 21, p. 35.
36. Fridman, Ya.D., *Okislitel'no-vosstanovitel'nye svoystva kompleksnykh soedinenii metallov i ikh ustoychivost' v rastvorakh* (Redox Properties of Complex Compounds of Metals and Their Stability in Solutions), Frunze: Ilim, 1966.
37. Yatsimirskii, K.B., *Zh. Neorg. Khim.*, 1970, vol. 15, no. 4, p. 925.
38. Fridman, Ya.D., Levina, M.G., Dolgashova, N.V., et al., *Ustoychivost' smeshannykh soedinenii v rastvorakh* (Stability of Mixed Compounds in Solutions), Frunze: Ilim, 1971.
39. Yatsimirskii, K.B., *Zh. Neorg. Khim.*, 1971, vol. 16, no. 3, p. 585.
40. Kravtsov, V.I., Krasikov, B.S., and Tsventarnyi, E.G., *Rukovodstvo k prakticheskim rabotam po elektrokhemii* (Manual of Laboratory Works on Electrochemistry), Leningrad: Len. Gos. Univ., 1979.
41. Lidin, R.A., Andreeva, L.L., and Molochko, V.A., *Konstanty neorganicheskikh veshchestv: Spravochnik* (Constants of Inorganic Substances: Reference Book), Moscow: Drofa, 2006.
42. Inczedy, J., *Analytical Applications of Complex Equilibria*, Budapest: Akad. Kiado, 1976.
43. Morachevskii, A.G., Voronin, G.F., Geiderikh, V.A., and Kutsenyuk, I.B., *Elektrokhimicheskie metody issledovaniya v termodinamike metallicheskh sistem* (Electrochemical Methods of Study in Thermodynamics of Metallic Systems), Moscow: Akademkniga, 2003.